Physics of the Northern Annular Mode -
Part 2: connection to meridional vorticity transfer

By Aarnout, J. van Delden
Institute for Marine and Atmospheric Research Utrecht (IMAU)
Physics Department, Utrecht University,
Princetonplein 5, 3584CC Utrecht, the Netherlands
a.j.vandelden@uu.nl
https://orcid.org/0000-0002-4980-5016

Version of 2 October 2023
Submitted for publication in Annals of Geophysics together with part 1 of this paper

Abstract

This is part 2 of two papers on the Northern Annular Mode (NAM). The NAM has two extreme phases. The negative NAM-phase is associated with an intense zonal-mean Sub-Tropical Jet (STJ) and a relatively deep, meridionally confined and intense baroclinic zone. Part 1 shows that the negative NAM-phase is maintained by intense poleward isentropic mass fluxes associated with the residual circulation in middle latitudes, and identifies a positive feeback loop between baroclinicity and the intensity of the residual circulation, which maintains the NAM in its negative phase. The positive NAM-phase is associated with a relative weak and meridionally broad zonal-mean Sub-Tropical Jet (STJ) associated with a relatively shallow and meridionally broad zonal-mean baroclinic zone. Part 2 investigates the different roles of eddies and mean meridional overturning circulation in middle latitudes, also known as the Ferrel circulation, in the meridional transfer of vorticity and mass in the positive feedback loop that sustains the positive NAM-phase. A very useful property of vorticity is that it behaves as the density of a substance called Potential Vorticity Substance (PVS). PVS is impermeable to isentropic surfaces. This is the reason why isentropic coordinates are adopted to study the feedback loops that maintain the NAM in an extreme phase. Very robust relations between PVS-fluxes due to eddies and PVS- and mass-fluxes due to the Ferrel circulation are found from re-analysis data in isentropic coordinates. Poleward eddy PVS-fluxes are in the lead in driving the positive NAM-phase, in particular in the latitude-band between 45°N and 55°N. This is because meridional eddy PVS-transfer in this latitude-band is directed up the meridional gradient of zonal-mean PVS. The positive NAM-phase is characterised by a relatively strong meridional PVS-gradient between 45°N and 55°N and hence also very intense poleward eddy PVS-fluxes at these latitudes. Meridional PVS fluxes due to eddies bring the westerlies out of gradient wind balance, hence forcing and, most important, broadening the Ferrel circulation in the poleward direction. In the upper troposphere and lowermost stratosphere the Ferrel circulation transfers mass toward the equator. This weakens the poleward residual isentropic mass flux in middle latitudes, hence perpetuating the positive NAM-phase, or preventing a transition to the negative NAM-phase.

1. Introduction

This paper is the second part of two papers that address the phenomenology and physics of the Northern Annular Mode (NAM), defined in detail in part 1 (van Delden, 2023). A viewpoint in isentropic coordinates is taken. The rather restrictive quasi-geostrophic approximation is avoided. The dynamical structure of the atmosphere is divided into the following three interacting components: **(1)** a "primary" zonally symmetric (i.e. zonal-mean) circumpolar circulation, **(2)** a "secondary" zonally symmetric *meridional* overturning circulation, consisting of the Hadley cells in the tropics and the Ferrel cells in the middle latitudes (Dima and Wallace, 2003), and **(3)** eddies and waves, or zonal asymmetries. These three components form the general circulation of the atmosphere.

The primary circulation is defined by the zonal-mean zonal wind velocity, $[u]$ (symbols are defined in the appendix to this paper). The secondary circulation is defined by the zonal-mean meridional wind velocity, $[v]$. Both $[u]$ and $[v]$ depend on time, latitude and height. Height in this paper is measured in terms of potential temperature,

$$\theta \equiv T\left(\frac{p_{ref}}{p}\right)^{\kappa}.$$

Meridional advective isentropic mass- and vorticity fluxes, associated with eddies and with the secondary circulation, are referred to in short, respectively, as *eddy fluxes* and *mean fluxes*. The sum of eddy- and mean fluxes is referred to as the *net flux*, or the *residual flux*, if the eddy flux is anticorrelated with the mean flux, which is quite usual, especially in the case of the meridional advective vorticity fluxes.

The NAM is identified with non-seasonal fluctuations in the primary circulation, specifically with coupled non-seasonal fluctuations of the strength of the zonal-mean Sub-Tropical Jet (STJ) and with the latitude of the maximum zonal-mean surface westerlies, associated sea-level pressure distribution. The negative NAM-phase, for example, is characterised by an intense zonal-mean STJ at the boundary between the tropical upper troposphere and the extratropical lowermost stratosphere, a very equatorward position of the most intense zonal-mean surface-westerlies, relatively weak sub-tropical high's in the Atlantic and Pacific Oceans and an intense and deep meridional residual circulation of mass. The aim here is to identify feedback-loops in the interaction of the three components of the general circulation that can maintain the NAM in an extreme phase for an appreciable time. What physical processes, for example, are involved in the feedback loop that sustains an intense STJ and simultaneously sustains weak subtropical highs?

Part 1 of this paper focuses on the role of meridional isentropic fluxes of mass in maintaining the NAM in its extreme negative phase. The persistence of the negative phase of the NAM is explained as due to a positive feedback-loop between baroclinicity below the STJ and the net meridional isentropic mass flux divergence just poleward of the STJ. This mass flux divergence is associated with eddies feeding on the available potential energy associated with baroclinicity below the STJ. This baroclinicity is strengthened by the meridional mass flux divergence in the upper poleward branch of the residual circulation of mass, thereby intensifying the baroclinic eddy activity and so also intensifying the associated mass flux divergence.

The present paper (part 2) provides further details of the driving of the NAM, and offers a physical explanation of the persistence of the positive phase of the NAM, which is characterised by a relatively weak zonal-mean STJ, a relatively weak and shallow zonal-mean baroclinic zone, a more poleward position of the most intense zonal-mean surface westerlies and a weak and shallow meridional circulation of mass.

Important findings and conclusions of part 1 of this paper are the following.

(1) The primary circulation, i.e. the zonal mean circumpolar flow, is in very close thermal wind balance. This means that the structure of the primary circulation, such as the strength of the STJ, depends on the zonal-mean potential vorticity (PV) distribution, in accord with a zonal-mean potential vorticity (PV) - inversion equation, which is an expression of zonal-mean thermal wind balance in terms of zonal-mean potential vorticity.

(2) A feature of the zonal-mean potential vorticity distribution that stands out is the positive PV-anomaly centred over the pole, approximately between the dynamical tropopause and the 370 K isentrope. This PV-anomaly, which is manifest principally as a negative isentropic density anomaly, defines the lowermost stratosphere. The STJ is found at the equatorward edge of this PV-anomaly in accordance with the solution of the zonal-mean PV-inversion equation.

(3) The positive PV-anomaly, defining the lowermost stratosphere, derives its identity from the fact that this layer has lost a large fraction of its mass, by cross-isentropic downwelling due to radiative flux divergence, to a dome of potentially cold air residing over the high latitude Northern Hemisphere.
(4) The intensity of the residual meridional mass flux fluctuates between intense phases and weak phases. The intense phase may consist of a series of mass flux pulses each lasting in order of 5 days.
(5) The intense and weak phases of the extratropical meridional circulation of mass are manifest at the earth's surface as a seesaw in pressure between the subtropical belt of high pressure and the relatively low pressure over the Polar Cap. The negative (positive) NAM phase is associated with a weakening (strengthening) of the zonal mean sea-level pressure gradient between subtropics and higher latitudes.

Part 1 of this paper does not answer the question how exactly the secondary circulation and eddies separately drive the primary circulation and associated zonal mean distribution of mass and vorticity. This question is the subject of this paper (part 2). Section 2 of this paper introduces the phenomenon of *planetary wave breaking* and the associated isentropic *potential vorticity mixing*. Section 3 explains the idea of vorticity as a substance, called *potential vorticity substance* (PVS), and derives a PVS-flux equation. The contributions to the advective PVS-flux due to, respectively, the secondary circulation and eddies are identified. From reanalysis data it is shown that advective PVS fluxes dominate the PVS-balance, but that this balance differs strongly in the respective extreme NAM-phases. In section 4 an equation is derived, which relates the time-rate of change of $[u]$ at a fixed latitude (i.e. the time-rate of change of the intensity of the primary circulation) to meridional advective fluxes of vorticity due to both the secondary circulation and eddies. Section 5 offers an explanation for the persistence of the positive phase of the NAM. Section 6 discusses the connection between the meridional eddy PVS flux and the meridional residual mass flux, which was shown, in part 1, to drive the negative phase of the NAM. Section 7 discusses a NAM-phase transition and demonstrates that the positive NAM phase is characterised by short planetary waves in middle latitudes, which propagate eastward relatively quickly, while slow eastward propagating long planetary waves characterise the negative NAM-phase. This paper is concluded in section 8.

2. Isentropic potential vorticity mixing due to breaking planetary waves

Figure 1 shows the evolution of the potential vorticity field and the zonal wind velocity on the 350 K isentropic surface in the Northern Hemisphere at 24-hour intervals, between 00 UTC on 13 December 2006 and 00 UTC on 15 December 2006. The 350 K isentropic surface intersects the STJ-core near the isentropic tropopause. Potential vorticity in isentropic coordinates (Z_θ) is defined as

$$Z_\theta \equiv \frac{\zeta_a}{\sigma}\ , \tag{1}$$

where the absolute vorticity is the sum of relative vorticity (ζ) and planetary vorticity (f),

$$\zeta_a \equiv \zeta + f\ , \tag{2}$$

and the isentropic density,

$$\sigma \equiv -\frac{1}{g}\frac{\partial p}{\partial \theta} \tag{3}$$

Vorticity and isentropic density are core variables in the understanding of the dynamics of the atmosphere. Other variables are defined in the appendix to this paper.

The following two regions of approximately uniform potential vorticity (PV) can be distinguished. The first region, shaded in red, in the tropics, is characterised by PV-values less than 1 PVU, while the second region, shaded in blue, in the extra-tropics, is characterised by much higher PV-values (5-8 PVU). By definition, the first region lies in the troposphere, while the second region lies in the lowermost stratosphere. The relatively narrow transition zone of strong isentropic PV-gradient in between encompasses the isentropic tropopause, which is usually identified by the 2 PVU isopleth of PV

(Ambaum, 1997) (1 PVU, or Potential Vorticity Unit, is equivalent to 10^{-6} s^{-1} kg^{-1} K m^2).

Under adiabatic conditions an air-parcel conserves its potential vorticity (PV) and remains on an isentropic surface. In **figure 1** we observe poleward intrusions of tropical (tropospheric) low-PV air and equatorward intrusions of extra-tropical (stratospheric) high-PV air on the 350 K isentropic surface. A tropical air mass can be identified at about 30°W (i.e. over the Eastern Atlantic Ocean), as it intrudes (moves poleward) into the middle latitudes. This intrusion represents the crest of a planetary wave, which appears to "break", like a breaking ocean wave.

The tropical low-PV air mass seems to return to the tropics following a clockwise (anticyclonic) trajectory, as if a "restoring force" is driving this low-PV air mass back to its "equilibrium position". In the case of ocean waves, gravity is responsible for the restoring force that drives the water parcels back to their equilibrium position. In **figure 1**, it appears as if an analogous "restoring force" is driving the tropical air back to the tropics. What is the origin of this mysterious "elasticity"? A hypothetical answer to this question is given in **section 3**. A more complete understanding of the source of this "elasticity" comes in **section 4**.

The crests of breaking planetary waves are associated with local jets, or "rapids" in the jet stream, called "jetstreaks", which move to relatively high latitudes (about 60°N), preferably over the North-Eastern Atlantic or Pacific Oceans, where these local jets are referred to as the "polar front jetstream".

Planetary waves are excited by (**1**) baroclinic instability, by (**2**) thermal (inertia) contrasts between continents and oceans, by **(3)** the interaction of the mean zonal flow with the inhomogeneous surface of the earth, and by (**4**) (sub-)tropical deep convection, especially over South East Asia (Indonesia). Enhanced wave activity in the form of breaking waves, forming closed eddies, is frequently observed at higher latitudes. This occurs in three preferred regions: (**1**) over the Eastern Pacific and adjacent Western North America, (**2**) over the Eastern Atlantic and adjacent Europe, and (**3**) over Japan.

Planetary wave breaking may appear as cyclonic wave breaking or as anticyclonic wave breaking (Bennedict et al., 2004). Anticyclonic planetary wave breaking, in which low-PV tropical air moves polewards and is deflected eastward, thus rotating anticyclonically, is observed in **figure 1** between the longitudes of 30°W and 30°E.

Potential vorticity (PV)-mixing at 350 K due to planetary wave breaking is reflected in the time-mean PV-distribution as a reduction of the isentropic meridional gradient of potential vorticity. The consequences of intense PV-mixing in middle latitudes in Janaury 2007 compared to weak PV-mixing iin middle latitudes in January 2010 are illustrated in **figure 2**. The much larger distance in the meridional direction between the 1 PVU and the 7 PVU isopleths in January 2007 than in January 2010 indicates that PV-mixing due to planetary wave breaking occurred over a larger range of latitudes in January 2007. The wave breaking was most frequently of the anti-cyclonic type in January 2007, occurring preferably in the North-East Pacific and Western Canada and over the North-East Atlantic and Europe, as is illustrated in **figure 1**. The associated frequent occurrence of jet streaks on the crest of the waves in January 2007 appears in the upper panel of **figure 2** as a second maximum in the frequency of the occurrence of high zonal wind speeds at high latitudes over the North-East Pacific Ocean and Western Canada (around longitude of -150° to -120°) and over the North-East Atlantic Ocean and Western Europe (around longitude of -40° to +30°), next to the frequency-maximum at lower (sub-tropical) latitudes. Although there is some indication of wave breaking and attendant PV-mixing at these longitudes in January 2010 (lower panel of **figure 2**), this is hardly associated with anticyclonic wave breaking, witness the relative absence of high zonal wind velocities at 350 K at high latitudes in January 2010.

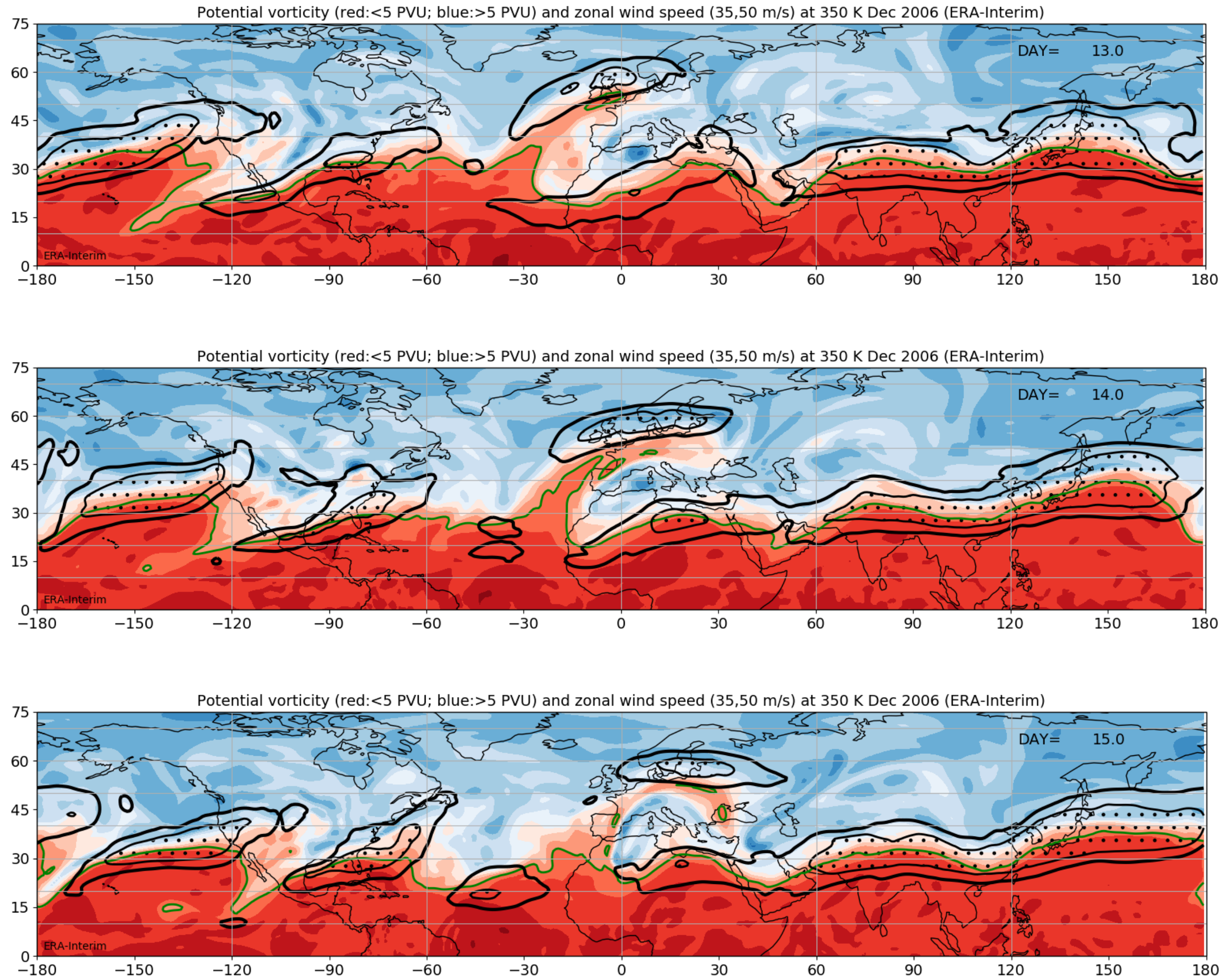

FIGURE 1. Potential vorticity (Z_θ) and zonal wind velocity (u) on the 350 K isentropic surface as a function of latitude (°N) (ordinate) and longitude (°E) (abscissa), at 00 UTC, 13 December 2006 (upper panel), 00 UTC, 14 December 2006 (middle panel), and at 00 UTC, 15 December 2006 (lower panel). Red shading corresponds to tropical air (Z_θ<5 PVU). Blue shading corresponds to extra-tropical air (Z_θ>5 PVU). The green contour is the isentropic dynamical tropopause_(Z_θ=2 PVU). Black contours of u are drawn for 35 m/s and 50 m/s. Dotted regions indicate that u>50 m/s. An ideal example of (anti-cyclonic) planetary wave breaking is observed between the longitudes of 30°W and 30°E, affecting the potential vorticity and zonal wind distributions in a band of latitudes between 30°N and 60°N. A "local jet", called a "jetstreak", with a length of several thousands of kilometers, is attached to the crest of the breaking wave. The subtropical jet consists of a series of jetstreaks, which are typically observed at the wave-crests, even when the wave-crest is not part of a breaking wave. Based on the ERA-Interim reanalysis (Dee et al., 2011).

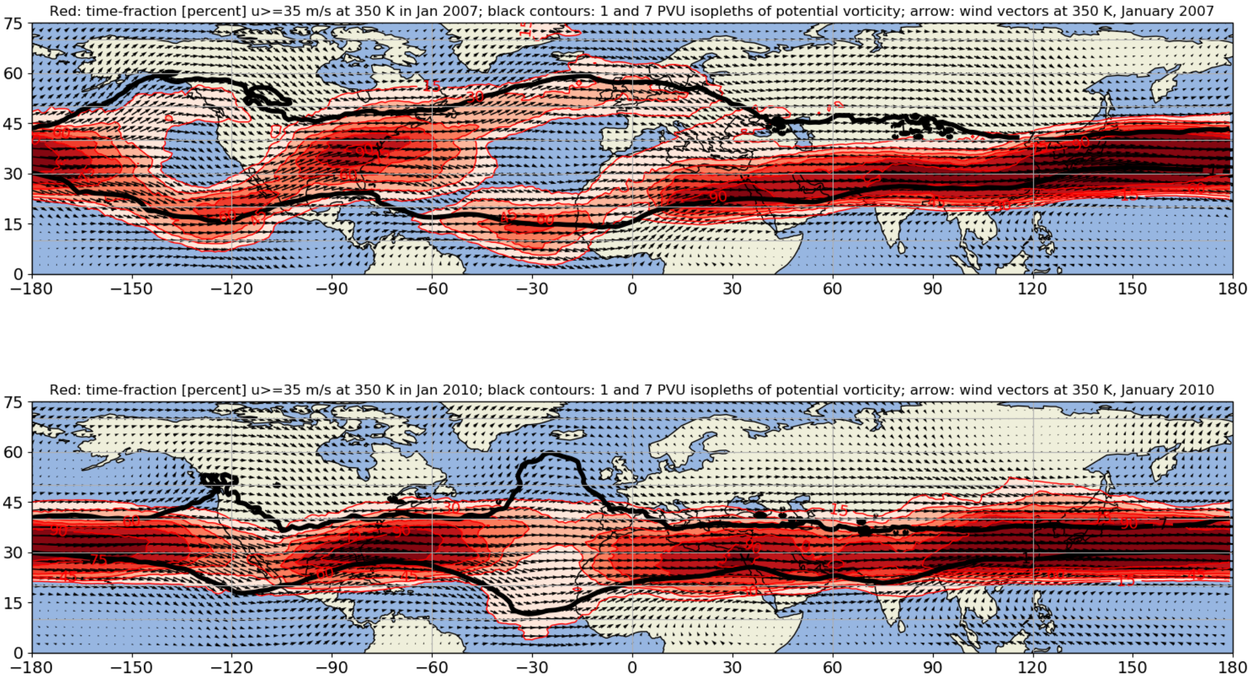

FIGURE 2. Fraction of time that the zonal wind velocity, u, exceeds 35 m s^{-1} (red contours and red shading) in January 2007 (upper panel) and in January 2010 (lower panel) as a function of latitude (°N) (ordinate) and longitude (°E) (abscissa). Contour-interval is 15%, starting at 15 %. Also shown are monthly mean wind vectors at θ=350 K, and the isopleths of monthly mean potential vorticity at θ=350 K corresponding to 1 PVU and 7 PVU. A large meridional distance between these isopleths indicates intense PV mixing by planetary wave breaking. Based on the ERA-Interim reanalysis (Dee et al., 2011).

3. Potential vorticity substance flux

The intensity of meridional PV-mixing due to planetary wave breaking is usually measured in terms of a meridional eddy-flux of potential vorticity. This, indeed, is the approach in the commonly adopted quasi-geostrophic theory in pressure coordinates. Quasi-geostrophic potential vorticity has the same dimension as vorticity (s^{-1}). If we choose to avoid the quasi-geostrophic approximation, and adopt isentropic coordinates, potential vorticity has the totally different dimension of $m^2Ks^{-1}kg^{-1} \equiv$ PVU. In isentropic coordinates, the potential vorticity (PV-) equation in flux form is found by combining the adiabatic advective potential vorticity equation,

$$\frac{\partial Z_\theta}{\partial t} + u\left(\frac{\partial Z_\theta}{\partial x}\right)_\theta + v\left(\frac{\partial Z_\theta}{\partial y}\right)_\theta = 0\ , \tag{1}$$

and the adiabatic mass-conservation equation (neglecting effects of the curvature of the earth),

$$\frac{\partial \sigma}{\partial t} + \left(\frac{\partial \sigma u}{\partial x}\right)_\theta + \left(\frac{\partial \sigma v}{\partial y}\right)_\theta = 0\ . \tag{2}$$

Multiplying (1) by σ, multiplying (2) by Z_θ, and adding the resulting equations yields the flux form of the PV-equation in isentropic coordiantes:

$$\frac{\partial \sigma Z_\theta}{\partial t} = -u\left(\frac{\partial \sigma Z_\theta}{\partial x}\right)_\theta - v\left(\frac{\partial \sigma Z_\theta}{\partial y}\right)_\theta - \sigma Z_\theta\left(\frac{\partial u}{\partial x}\right)_\theta - \sigma Z_\theta\left(\frac{\partial v}{\partial y}\right)_\theta = -\left(\frac{\partial u\sigma Z_\theta}{\partial x}\right)_\theta - \left(\frac{\partial v\sigma Z_\theta}{\partial y}\right)_\theta \tag{3}$$

which, in fact, is nothing else than the flux form of the vorticity equation:

$$\frac{\partial \zeta_a}{\partial t} = -\vec{\nabla}\cdot\vec{J}\ , \tag{4}$$

with the *advective vorticity flux vector* defined as

$$\vec{J} \equiv \left(u\zeta_a,\ v\zeta_a,\ 0\right)\ . \tag{5}$$

Note the analogy between eq. 4 and eq. 2, which can be written in short as

$$\frac{\partial \sigma}{\partial t} = -\vec{\nabla}\cdot\vec{I}\ , \tag{6}$$

where the adiabatic mass flux vector is

$$\vec{I} \equiv \left(u\sigma,\ v\sigma,\ 0\right)\ . \tag{7}$$

To continue the analogy between (4) and (6) and between (5) and (7), it may be said that absolute vorticity is equivalent to the *density* (or *concentration*) of a fictitious substance, which is called “Potential Vorticity Substance” (“PVS”) (Haynes and McIntyre, 1987, 1990). Potential vorticity, which, in contrast to PVS, is materially conserved, can be regarded as the “mixing ratio of PVS”, because it is defined as “PVS-density divided by total mass-density”.

The analogy of PVS with a substance is a valuable way of interpreting the dynamical behaviour of the atmosphere, but we should be aware of the following two caveats of this interpretation (Haynes and McIntyre (1987); **(1)** the mixing ratio of PVS is not a dimensionless quantity, as is the mixing ratio of real chemical substance, such as water vapour, and **(2)** unlike the amount of a real chemical substance, the “amount of PVS” may be negative.

Because eqs. 4 and 5 assume adiabatic (isentropic) conditions, it is no surprise that the PVS-flux, $\vec{J}$, has no component across an isentropic surface (eq. 5). However, very remarkably, this is also true in nonadiabatic conditions (Haynes and McIntyre, 1987, 1990), but with the PVS-flux vector, $\vec{J}$, defined by

$$\vec{J} \equiv \left(u\zeta_a + \frac{d\theta}{dt}\frac{\partial v}{\partial \theta} - F_y, \, v\zeta_a - \frac{d\theta}{dt}\frac{\partial u}{\partial \theta} + F_x, \, 0 \right) \quad , \tag{8}$$

instead of by eq. 5. In (8), F_x and F_y are the x-component and y-component, respectively, of arbitrary frictional forces per unit mass. According (8), isentropes are impermeable to PVS, even when mass crosses isentropic surfaces due to, for example, radiative flux divergence, and even in the presence of arbitrary frictional forces! This statement is known as the "Impermeability theorem for potential vorticity substance".

By definition, isentropic surfaces above the Underworld do not have side-boundaries. Therefore, the global integral of PVS (or absolute vorticity) on an isentropic surface in both the Middleworld and the Overworld is constant, equal to zero, mostly negative in the Southern Hemisphere and mostly positive in the Northern Hemisphere.

Let us calculate the zonal mean advective meridional flux of PVS from reanalysis data. For this, we introduce the following definitions. The zonal mean, i.e. the average of any variable around a full latitude circle, indicated by brackets, in this case of the meridional velocity and of the absolute vorticity, respectively, is defined as

$$[v] \equiv \frac{1}{2\pi}\int_0^{2\pi} v \, d\lambda \text{ and } [\zeta_a] \equiv \frac{1}{2\pi}\int_0^{2\pi} \zeta_a \, d\lambda \ . \tag{9}$$

Any variable is expressed as a sum the zonal mean value and a perturbation, indicated by an asterisk, as

$$v = [v] + v^* \text{ and } \zeta_a = [\zeta_a] + \zeta^* . \tag{10}$$

(note that $\zeta_a^* = \zeta^*$). The zonal mean advective meridional flux of PVS is

$$\boxed{[v\zeta_a] \equiv \left[([v]+v^*)([\zeta_a]+\zeta^*)\right] = \left[[v][\zeta_a] + v^*[\zeta_a] + [v]\zeta^* + v^*\zeta^*\right] = [v][\zeta_a] + \left[v^*\zeta^*\right]} \ . \tag{11}$$

Eq. 11 demonstrates that the total meridional flux of PVS is the sum of a so-called "*mean*" contribution, $[v][\zeta_a]$, due to the secondary meridional overturning circulation, and a so-called "*eddy*" contribution, $[v^*\zeta^*]$, due to zonally asymmetric part of the flow, i.e. due to eddies. The former contribution is henceforth referred to as the *mean* PVS-flux, while the latter contribution is referred to as the *eddy* PVS-flux.

The time-integrated net meridional advective flux of PVS (ΔF) after $t=t_0$ is defined as,

$$\Delta\mathrm{F}(t) = \int_{t_0}^{t} [v\zeta_a] \, dt \quad [\mathrm{m\ s^{-1}}] \ . \tag{12}$$

Figure 3 shows the daily running mean *mean* PVS-flux, $[v][\zeta_a]$, (thick red line) and the daily running mean *eddy* PVS-flux, $[v^*\zeta^*]$, (thin red line) at 50.25°N and θ=350 K, between 1 December 2006 and 28 February 2007 (upper panel), and between 1 December 2009 and 28 February 2010 (lower panel), based on the ERA-Interim reanalysis data with a resolution of 0.75° in space and 6 hours in time. The black line represents ΔF. The parameter, t_0, in eq. 12 is set to 1 December 2006, 00 UTC (upper panel), and to 1 December 2009, 00 UTC (lower panel). To calculate time-integrated fluxes it is assumed that the fluxes are constant over six-hour intervals.

Note in **figure 3** that the *eddy* PVS-flux ($[v^*\zeta^*]$) and the *mean* PVS-flux ($[v][\zeta_a]$) seem to compensate each other in both winters, i.e. they are anti-correlated. This compensation of eddy- and mean-advective meridional fluxes may explain the "mysterious elasticity", discussed earlier in section 2. This point will be discussed and explained further in **section 4**.

Note also in **figure 3** that ΔF and $[u]$ are highly correlated in both winters. The zonal-mean zonal wind velocity, $[u]$, at the 50.25°N-parallel, apparently, is determined by the net meridional advective PVS-flux across this same parallel. This can be understood easily from the circulation theorem and Stokes theorem, which relates the integral around a closed curve of the component of the velocity vector parallel to this closed curve to the mean vorticity within the area enclosed by this curve. Therefore, the time-integrated total flux of vorticity (PVS) across any parallel, which is a closed curve, determines the change in $[u]$ at that same parallel. The almost perfect correlation of the time-integrated *advective* flux ΔF (the black curve) and $[u]$ (the blue curve) indicates that the diabatic and frictional contributions to the net PVS-flux (eq. 8) are negligible over the period in question (three winter months). Evidence of this fact is presented in section 4. The slight systematic divergence of the black and blue curves over a period of 3 months, as displayed in **figure 3**, is very probably due to the diabatic contribution to the flux of PVS (the term containing $d\theta/dt$ in eq. 8).

The meridional advective PVS-flux may be interpreted as a zonal force per unit mass, similar to F_x in eq. 8. A poleward isentropic PVS-flux in the Northern Hemisphere is equivalent to an eastward force per unit mass and an associated eastward "acceleration" of the mean speed of air on a closed parallel. The *eddy* isentropic PVS-flux, $[v^*\zeta^*]$, at 50°N and at 350 K in the winter of 2006-2007 (the thin red line in the upper panel of **figure 3**), is positive (poleward) almost all the time. Therefore, eddies contribute to a continuous increase of the area-average vorticity over the Polar Cap (poleward of 50.25°N), implying that eddies act to intensify the zonal-mean zonal eastward wind at 50.25°N! Hence we say that the westerlies at 60°N (at θ=350 K) are "eddy-driven".

However, things are not always this way. In the winter of 2009-2010 the eddy isentropic PVS-flux at 50°N and at 350 K is equatorward during two time-intervals each lasting about 5 days, which, *singly*, would lead to a weakening of the eastward zonal current at the same latitude. This effect of eddies on the zonal-mean zonal wind is sometimes interpreted by saying that "the zonal-mean zonal wind is weakened due to planetary wave drag" (page 869 of Plumb and Eluszkiewicz, 1999; page 162 of Butchart, 2014).

The next section gives further mathematical details of the physics behind the relation between meridional PVS-fluxes and intensification or weakening of the westerlies.

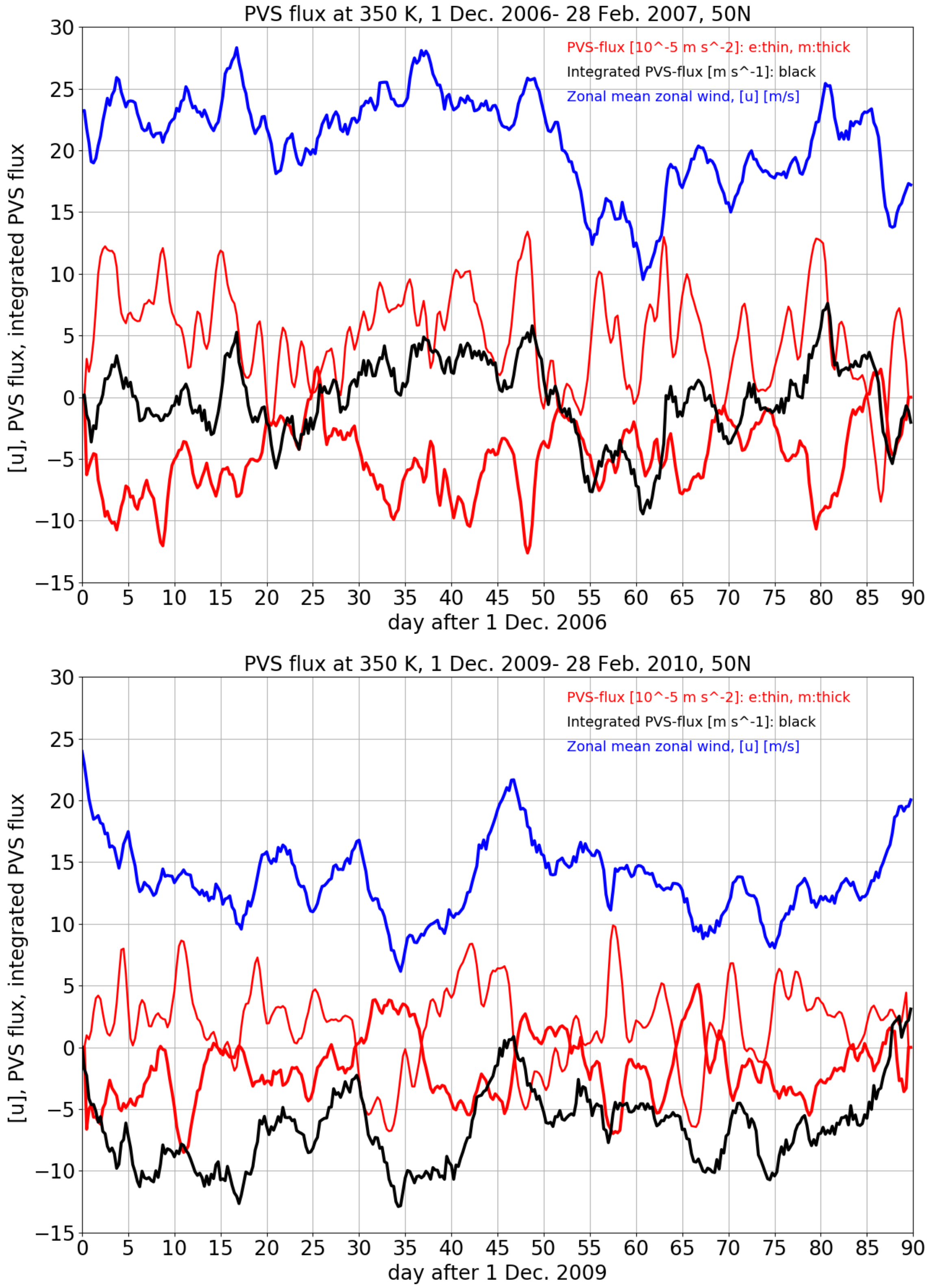

FIGURE 3: Meridional isentropic PVS-flux at ϕ=50.25°N and θ=350 K (lowermost stratosphere), between 1 December 2006 and 28 February 2007 (upper panel) and between 1 December 2009 and 28 February 2010 (lower panel). The thick red line represents the running daily mean flux due to the secondary circulation ($[v][\zeta_a]$), while the thin red line represents the running daily mean flux flux due to eddies ($[v^*\zeta^*]$). The black line represents the time integrated net (cumulative) flux of PVS ($\Delta F(t)$) (upper panel) after 1 December 2006 (00 UTC), defined in eq. 1.235. The blue line represents the zonal-mean zonal wind, $[u]$, at ϕ=50.25°N. Based on the ERA-Interim reanalysis (Dee et al., 2011).

4. Intensification or weakening of the zonal-mean westerlies

Section 3, in particular **figure 3**, demonstrates that the zonal-mean zonal wind, $[u]$, at a specified latitude (in this case, 50.25°N) and isentropic level (in this case 350 K) is mostly "accelerated" in eastward direction due to the meridional *eddy* PVS-flux, $[v^*\zeta_a^*]$, at that same latitude. Because we are not referring to a material time-derivative of $[u]$, it is more correct to say, "intensified" instead of "accelerated". **Figure 3** also demonstrates that the meridional *eddy* PVS-flux is almost exactly countered by the *mean* PVS-flux, $[v][\zeta_a]$. If the *mean* PVS-flux is equatorward it is part of the upper horizontal leg of the secondary Ferrel circulation. The secondary Ferrel circulation in middle latitudes exists in order to maintain the atmosphere in, or close to, zonal-mean thermal wind balance (Eliassen, 1951; Kuo, 1956). In other words, due to the Ferrel circulation, zonal-mean zonal winds are never strongly super-gradient or strongly sub-gradient.

The compensation between eddy- and mean- meridional fluxes of vorticity is never exact. The linear regression in **figure 4** of part 1 of this paper (van Delden, 2023) suggests that in January, $[u_{gr}] = -0.25 + 0.99[u]$ at 50°N and θ=315 K (upper troposphere) and that $[u_{gr}] = -1.78 + 1.01[u]$ at 30°N and θ=350 K (near the core of the STJ). Actual zonal-mean winds are always super-gradient ($[u]>[u_{gr}]$) *at these latitudes* and *levels*. This, however, is no more than a statistical result. We do not understand its physical background!

This section derives an equation, based on physics, which directly relates the meridional fluxes of vorticity to the time rate of change of the zonal-mean zonal wind. The derivation starts with the *x*-component of the momentum equation in isentropic coordinates (Dutton, 1976, eqs. 53). Neglecting the curvature term, which is important only at high latitudes (>75°), and for high wind speeds (>100 m s^{-1}), this momentum equation is as follows.

$$\frac{\partial u}{\partial t} + u\frac{\partial u}{\partial x} + v\frac{\partial u}{\partial y} + \frac{d\theta}{dt}\frac{\partial u}{\partial \theta} = -\frac{\partial \Psi}{\partial x} + fv \,. \tag{13}$$

With the definition of relative vorticity (again neglecting the effect of earth's curvature),

$$\zeta = \frac{\partial v}{\partial x} - \frac{\partial u}{\partial y} \,, \tag{14}$$

and assuming adiabatic conditions ($d\theta/dt=0$), eq. 13 becomes

$$\frac{\partial u}{\partial t} = -\frac{1}{2}\frac{\partial}{\partial x}\left(u^2\right) - \frac{1}{2}\frac{\partial}{\partial x}\left(v^2\right) + v\zeta - \frac{\partial \Psi}{\partial x} + fv \,. \tag{15}$$

Taking the zonal mean, indicated by square brackets (defined in **section 3**), of eq. 15 yields

$$\frac{\partial [u]}{\partial t} = [v\zeta] + f[v] \,. \tag{16}$$

The first term on the r.h.s. of eq. 16 is divided into a part associated with the secondary circulation ($[v]$) and a part associated with the zonal asymmetries (eddies), as in eq. 10. This yields

$$\frac{\partial [u]}{\partial t} = [v]([\zeta] + f) + [v^*\zeta^*] \,. \tag{17}$$

According to eq. 17, the time-rate of change of the zonal-mean zonal wind at a specified latitude is determined by the zonal-mean net advective meridional vorticity-flux at that same latitude. This vorticity flux consists of the following two terms: (**1**) the zonal-mean meridional absolute vorticity flux due to the secondary circulation (first term on the r.h.s. of 17), and (**2**) the zonal-mean eddy vorticity flux (second term on the r.h.s. of 17). **Figure 4** (left panel) demonstrates that the intensification or weakening of the zonal-mean eastward wind over 24-hour intervals in the month of January 2007 are determined almost fully by the net advective and adiabatic meridional vorticity-flux over identical intervals. The slight difference between the zonal-mean eastward wind intensification and the advective vorticity-flux is explained by the likely small diabatic contribution to the vorticity-flux (eq. 8), or PVS-flux, and by the fact that the zonal-mean eastward wind intensification is evaluated using the following linear approximation to the time derivative:

$$\left(\frac{\partial[u]}{\partial t}\right)_n \approx \frac{[u]_{n+2}-[u]_{n-2}}{4\Delta t} \ , \tag{18}$$

where n is the index of time and Δt is the time step or resolution in time of the data (6 hours), and by the fact that the PVS-flux, $\overline{F}_n$, averaged over an interval of 24 hours, is evaluated according to the approximation,

$$\overline{F}_n = \left(F_{n-2} + (2\times F_{n-1}) + (2\times F_n) + (2\times F_{n+1}) + F_{n+2}\right)/8 \,. \tag{19}$$

While exact equilibrium ($\partial[u]/\partial t$=0) is hardly ever observed over a 24-hour period (right panel of **figure 4**), near-equilibrium is indeed observed over a period of one month. In other words, the *mean* meridional advective PVS-flux is approximately equal and opposite to the *eddy* meridional advective PVS-flux, as follows:

$$\int_0^\tau \left([v]([\zeta]+f)\right)dt \approx \int_0^\tau \left(-[v^*\zeta^*]\right)dt \,, \tag{20}$$

if τ=1 month. **Figure 5** demonstrates that the equilibrium, expressed by eq. 20, is valid to a very high degree at 50°N and 315 K for all months of January. This equilibrium, however, *differs quantitatively* in January of different years, with the months of January 2007 (**red dot**) and January 2010 (**blue dot**) as extremes. On average, eddies *intensify* the zonal-mean eastward flow at 50°N by about 6×10^{-5} m s^{-2} in January 2007, while eddies *weaken* the zonal-mean eastward flow at 50°N by nearly 2×10^{-5} m s^{-2} in January 2010.

Examining the two terms, which make up the net advective PVS-flux, in a large range of latitudes and levels in the Northern Hemisphere, we find that eddies *intensify* the zonal-mean eastward flow in a broad range of middle latitudes, especially in the lowermost stratosphere (left panels of **figure 6**). The equatorward boundary of the latitude-band, where eddies intensify the eastward zonal-mean flow, coincides approximately with latitude of the STJ at 30°N. The latitude of the poleward boundary of the latitude-band, where eddies intensify the eastward zonal-mean flow, on the other hand, is very variable. In January 2007, for example, it is located relatively far poleward at 60°N (upper left panel of **figure 6**), while in January 2010 it is located less far poleward at 50°N (lower left panel of **figure 6**l).

In January 2007, the monthly mean *eddy* PVS-flux peaks at just over 8×10^{-4} m s^{-2} at 50°N and 330 K (250 hPa). This would intensify the zonal-mean eastward flow by about 7 m s^{-1} per day if it were not countered almost exactly by the PVS-flux due to the secondary circulation (right panels of **figure 6**). The monthly mean eddy PVS-flux in January 2010 peaks at a similar value, but more southward, just south of 40°N, and somewhat higher at 350 K (200 hPa).

Weakening of the zonal-mean eastward wind *by eddies*, occurs in the tropics and over the Polar cap. The zonal-mean zonal wind in the upper branch of the winter Hadley cell, for example, is significantly weakened by tropical eddies. The Hadley circulation, therefore, is far less zonally symmetric than is suggested by the habitual schematic view of this circulation in many elementary standard textbooks.

The right panels of **figure 6** demonstrate that the monthly average meridional *mean* PVS-flux (due to the secondary circulation) almost exactly counteracts the monthly average *eddy* PVS-flux at most levels and latitudes. This implies that zonal-mean eastward wind "intensifications" over periods of one month are very small, relative to zonal-mean eastward wind "intensifications" over periods of one day, as is demonstrated also in **figures 4** and **5**. This also supports the idea that the secondary circulation exists in order to maintain approximate zonal-mean geostrophic (or gradient wind) balance in the face of "eddy-driving" of the zonal-mean zonal wind, especially in the mid-latitudes.

In the mid-latitudes the secondary circulation represents the "ageostrophic response" to eddy-driving. While the time-average *eddy* PVS flux is compensated almost exactly by the time-average *mean* PVS flux on a monthly time-scale, as can be seen in **figures 5** and **6**, this is not the case on the daily time-scale (right panel of **figure 4**). At 50.25°N and 315 K daily average *eddy* PVS fluxes much larger than the monthly average of +6 m s^{-2} are accompanied by much weaker than average daily average *mean* PVS fluxes in the opposite direction and vice versa.

The ageostrophic response is presumably an important reason for the apparent "elasticity" of breaking planetary waves (**figure 1**), alluded to in **sections 2** and **3**. In the example shown in **figure 1**, the ageostrophic response drives the tropical air mass, which is characterised by low potential vorticity, and which has penetrated into the higher middle latitudes, forming the crest of a planetary wave, back to the latitude of origin. The close balance between the *eddy* PVS-flux (driving the zonal mean state away from balance) and the *mean* PVS-flux (driving the zonal mean state back to balance) is a manifestation of "**geostrophic turbulence**", a term coined by Jules Charney (1971).

It is interesting to note that *weakly negative* daily average advective *eddy* PVS-fluxes are not always compensated by positive daily average advective *mean* PVS-fluxes (right panel of **figure 4**), implying that eddies and the secondary circulation may in such circumstances cooperate to weaken the zonal-mean zonal wind at 50°N and so drive the NAM away from its positive phase into the negative phase.

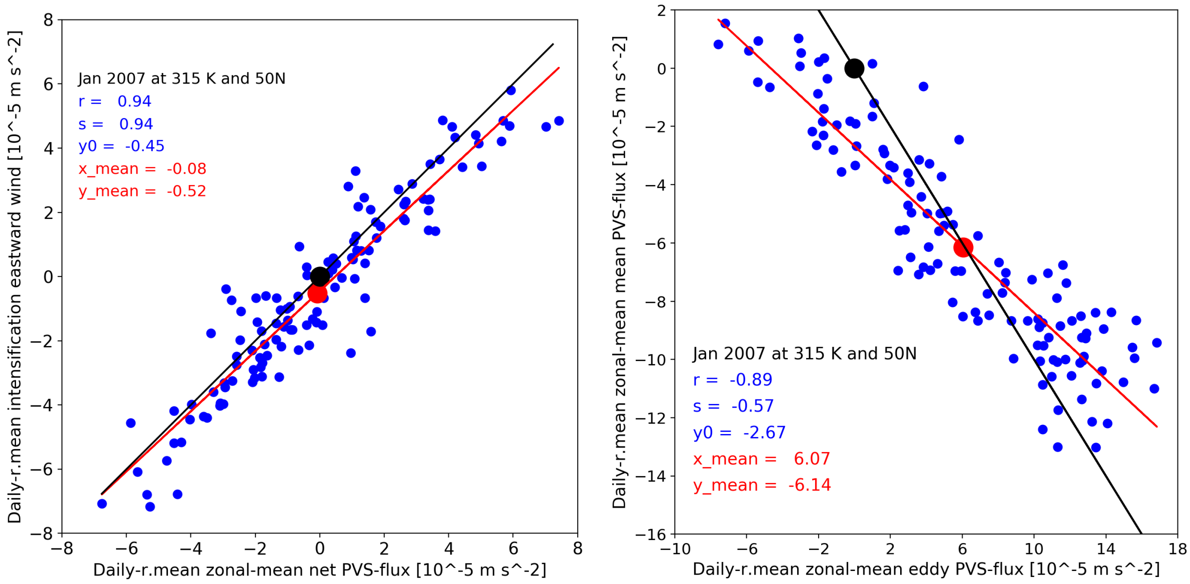

FIGURE 4. **Left panel**: time-rate of change of the eastward zonal-mean zonal wind, $\partial[u]/\partial t$ (l.h.s. of eq. 1.292), at 50°N and θ=315 K over 123 overlapping 24-hour intervals (running mean shifted by intervals of 6 hours) in January 2007 as a function of the zonal-mean net advective isentropic vorticity (PVS) flux (r.h.s. of eq. 1.292), averaged over the corresponding 24-hour intervals. **Right panel**: the zonal-mean *mean* meridional PVS-flux as a function of the zonal-mean *eddy* meridional PVS-flux at 50°N and θ=315 K over all 123 partly overlapping 24-hour intervals in January 2007. The red straight line in both panels represents the best linear fit. The associated correlation coefficient, r, and slope, s, are indicated. The large red dot represents the monthly average. The black straight line in both panels has a slope, s=1, and intersects the origin (black dot). On a 24-hour time-scale, eddies are in the lead in intensifying or weakening the zonal-mean eastward wind at 50°N, while the meridional overturning circulation usually opposes the effect of eddies, but never exactly. The red straight line converges towards the black "one-to-one" line with increasing averaging time. Based on the ERA-Interim reanalysis (Dee et al., 2011).

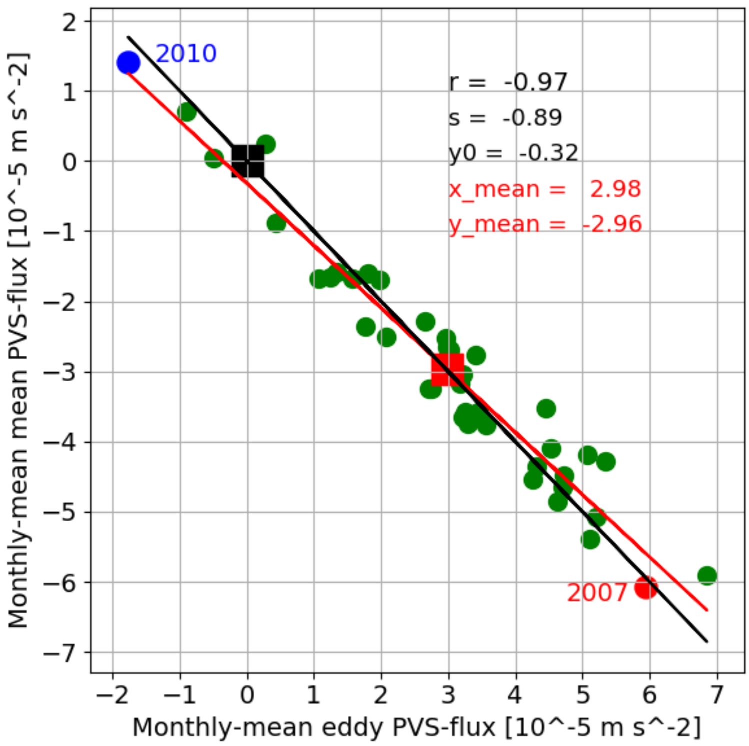

FIGURE 5. Scatter plot of the monthly average zonal-mean ***mean*** isentropic PVS-flux, $[v][\zeta_a]$, as a function of the monthly average zonal-mean ***eddy*** isentropic PVS-flux, $[v^*\zeta^*]$, at 315 K and 50°N, for all months of January between 1979 and 2018. The black straight line has slope, s=1, and intersects the origin, indicated by the black square. The red straight line represents the best linear fit to the 40 points (correlation coefficient is -0.97). The slope of this line is s= -0.89 and crosses the y-axis at y=-0.32×10^{-5} m s^{-2}. The large red square represents the ensemble average value for all 40 months of January. The ensemble average eddy PVS-flux ($+2.98\times10^{-5}$ m s^{-2}) is in close balance with the ensemble average mean PVS-flux (-2.96×10^{-5} m s^{-2}). The blue dot is for January 2010 (extreme negative NAM phase); the red dot is for January 2007 (extreme positive NAM phase) (section 1.27). Based on the ERA-Interim reanalysis (Dee et al., 2011).

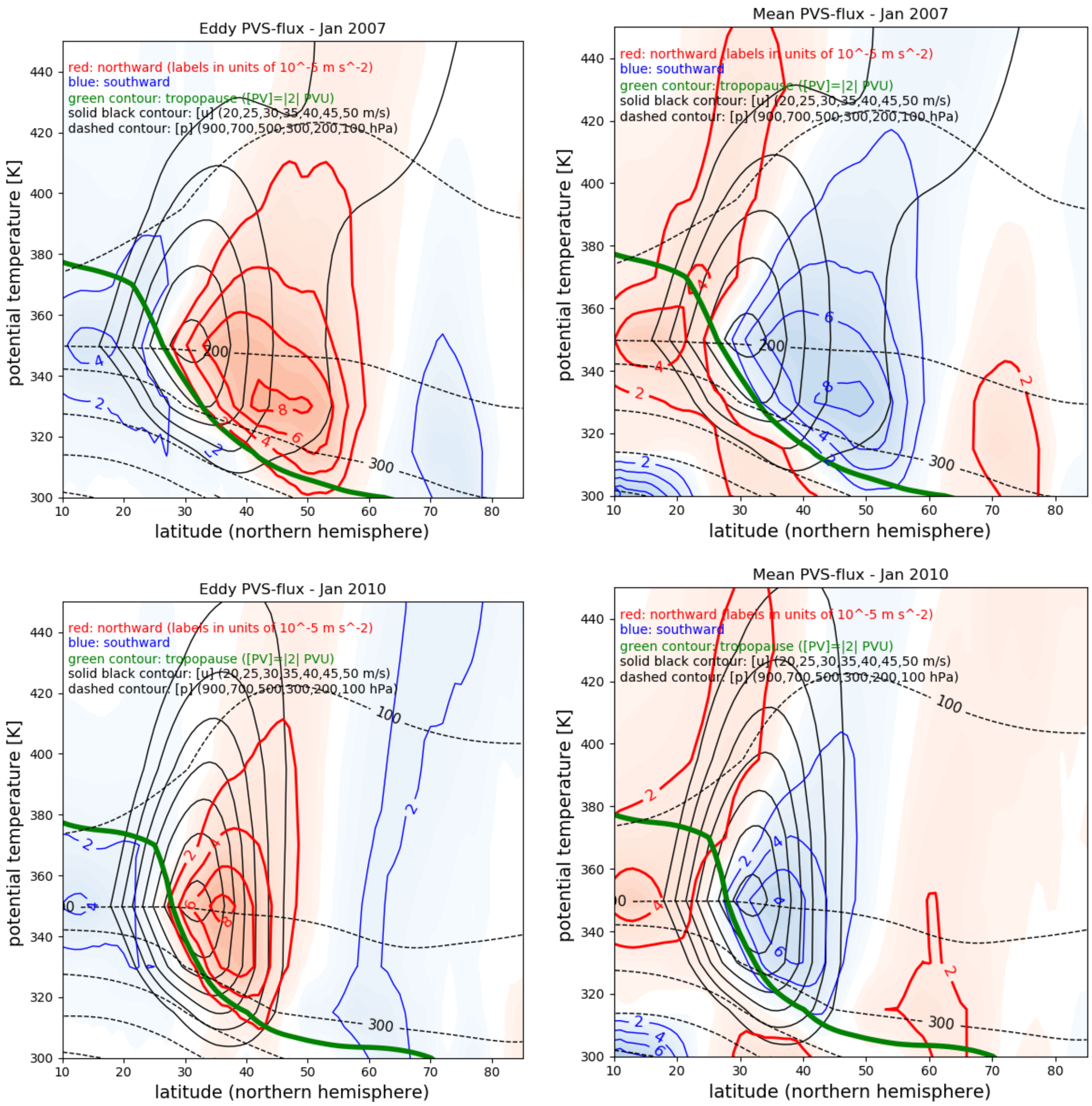

FIGURE 6. Monthly mean, zonal-mean isentropic PVS-flux as a function of latitude and potential temperature in January 2007 (upper panels) and in January 2010 (lower panels). **Left panels**: eddy PVS-flux, $[v^*\zeta^*]$. **Right panels:** PVS-flux, $[v][\zeta+f]$, due to the mean meridional circulation. Red shading corresponds to northward PVS-fluxes, which in adiabatic circumstances should lead to an intensification of the zonal-mean eastward wind. Blue shading corresponds to southward PVS-fluxes, which in adiabatic circumstances should lead to a weakening of the zonal-mean eastward wind. Labels are in units of 10^{-5} m s^{-2}. Also shown are the monthly mean, zonal mean pressure (dashed contours) (labeled in hPa), **the** dynamical tropopause (green contour) (2 potential vorticity units) and the zonal-mean zonal wind velocity (black solid contours, starting at 20 m s^{-1} at 5 m s^{-1} intervals. The poleward edge of the region of poleward eddy PVS-fluxes in middle latitudes, which presumable reflects the poleward edge of anticyclonically breaking planetary waves (**figure 1**), is found at a higher latitude in January 2007 (at about 60°N) than in January 2010 (at about 50°N). Based on the ERA-Interim reanalysis (Dee et al., 2011).

5. Eddy PVS-fluxes are up-gradient and therefore self-sustaining

It is an every-day observation that mixing by turbulent eddies of a materially conserved quantity, which is initially distributed inhomogeneously, ends with complete homogenisation of the concentration of this substance in the mixing-zone, and, therefore, also to cessation of the associated "down-gradient" turbulent fluxes in the mixing-zone. This observation translates into the hypothesis that the turbulent flux of a materially conserved quantity is directed down the mean spatial gradient of its *concentration*. More mathematically, this hypothesis states that the turbulent flux, $\vec{J}$, of a materially conserved quantity is proportional to the spatial gradient of its concentration, φ, as

$$\vec{J} = -D\vec{\nabla}\varphi \ .$$

Here, D is a *positive* eddy diffusion coefficient, i.e. the flux is proportional to the negative of the concentration gradient. This is an expression of Fick's law. A down-gradient turbulent flux of a substance acts to reduce the gradient of the concentration of this substance and so also to reduce the flux of this substance.

Do eddy PVS-fluxes obey Fick's law? To find an answer to this question, we first recapitulate the following conclusion of Haynes and McIntyre (1987, 1990). In isentropic coordinates, vorticity is the same as the *concentration* (amount per unit volume) of a substance, called "Potential Vorticity Substance" (PVS). If we divide PVS-concentration (i.e. vorticity) by mass concentration, or isentropic mass density (σ), we retrieve the *mixing ratio of PVS*, which is nothing else than potential vorticity, which is materially conserved in adiabatic circumstances.

Figure 7 demonstrates that the monthly mean meridional *flux of PVS-concentration* due to eddies in the atmosphere approximately obeys Fick's law *only* if the associated diffusion coefficient, D, is negative! The linear regression shown in **figure 7** (the red line) suggests that the meridional eddy flux of PVS-concentration is *positively* correlated with the meridional gradient of PVS-concentration. The poleward eddy PVS-flux, therefore, acts to increase the meridional gradient of PVS, and hence also acts to further intensify the poleward eddy PVS-flux. Victor Starr (1909-1976), who stood at the forefront of early studies of large-scale atmospheric transfer phenomena, became so acutely aware of this unusual flux-gradient relationship that he felt obliged to write a book on this topic, entitled "*Negative Viscosity Phenomena*" (Starr, 1968).

Numerical simulations of baroclinic planetary wave life-cycles (Balasubramanian and Garner, 1997; Thorncroft et al., 1993) have shown that the trough and ridge lines in the horizontal plane of planetary waves in the Northern Hemisphere have the propensity to tilt forward from south-west to north-east, due to the meridional gradient of the planetary vorticity, $\beta = \mathrm{d}f/\mathrm{d}y$, which is proportional to the cosine of latitude. A forward wave-tilt promotes anticyclonic wave breaking, as in the case shown in **figure 1**. A forward wave-tilt also means that $[u^*v^*]>0$, implying that westerly momentum in the Northern Hemisphere is transferred poleward and must converge at higher latitudes, usually between 50°N and 60°N, thus intensifying the zonal-mean zonal wind at these higher latitudes (see figure 1 of Starr, 1948). Converging westerly momentum fluxes and poleward vorticity transfer are theoretical manifestations of an identical process (Kuo, 1951). The vorticity flux-gradient relationship, shown in **figure 7**, indicates that we can generalise the conclusions of the above-mentioned numerical experiments to the meridional gradient of the *absolute* vorticity associated with both β *and* the relative vorticity of the flow in the background of the waves. At 50°N, the planetary vorticity-gradient, $\beta = 14.7\times10^{-12}$ m^{-1}s^{-1}. The monthly-mean meridional gradient of *absolute* vorticity between 45 and 55°N, at 330 K, is greater than β in 9 out of 41 months of January between 1979 and 2019. Among these 9 months is January 2007, characterised by a very intense poleward eddy vorticity flux. On the other side of the spectrum is January 2010, in which a very weak, although still positive, monthly-mean meridional gradient of absolute vorticity between 45 and 55°N is paired to a very weak monthly-mean poleward eddy vorticity flux.

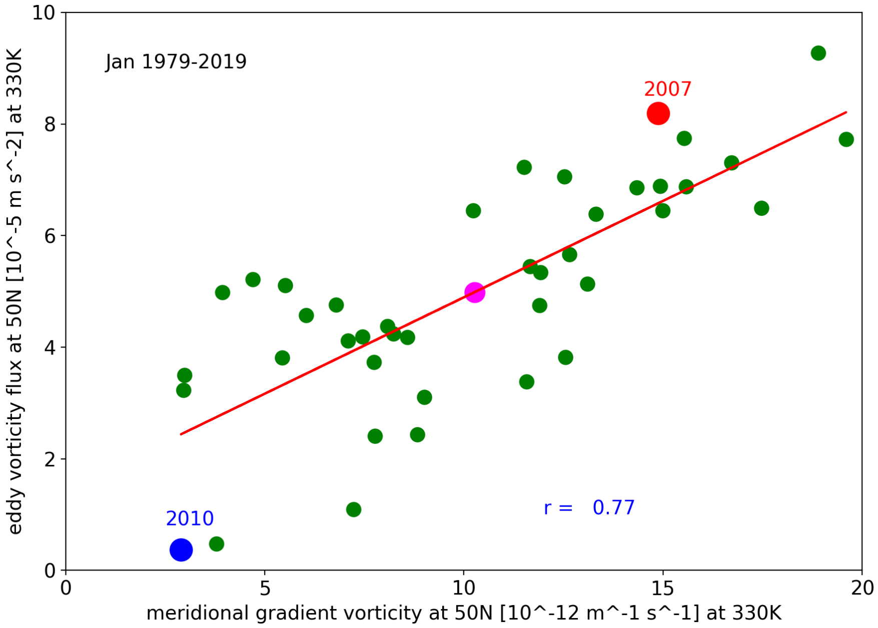

FIGURE 7. Scatter plot of the monthly-mean and zonal-mean eddy flux of PVS, $[v^*\zeta_a^*]$, at θ=330 K and 50°N, in January (1979-2019), and the corresponding zonal mean meridional gradient of monthly-mean absolute vorticity, at θ=315 K at 50°N, calculated by taking the difference of the absolute vorticity at 45°N and 55°N and dividing by the distance between these two parallels. The meridional gradient of planetary vorticity at 50°N is β=14.7×10^{-12} m^{-1}s^{-1}. The meridional gradient of absolute vorticity at 50°N is always positive. The red dot represents January 2007 (extreme positive NAM-index). The blue dot represents January 2010 (extreme negative NAM-index). The magenta dot represents January ensemble average for the years 1979-2019**.** The correlation coefficient, r, of the linear fit (the red line) to the 41 data points is 0.77. Based on the ERA-Interim reanalysis (Dee et al., 2011).

6. The role of meridional eddy PVS-fluxes in sustaining the positive NAM-phase

Meridional *eddy* PVS-fluxes in middle latitudes mostly intensify the primary circulation, thereby driving the atmosphere away from zonal-mean gradient wind balance. This imbalance in the meridional direction generates a secondary meridional overturning circulation in middle latitudes, which is referred to as the "Ferrel cell". Due to the Ferrel cell, the primary circulation is maintained in close gradient wind balance., as was first demonstrated by Eliassen (1951) and Kuo (1956).

The Ferrel cell extends further polewards during the positive NAM-phase than during the negative NAM-phase. This fact was noted first by Li and Wang (2003). This fact is verified in the right panels of **figure 6**, in the case of January 2007 (positive NAM-phase; upper right panel) and January 2010 (negative NAM-phase; lower right panel). The Ferrel cell in January 2007 extends roughly from 30°N to 60°N, while the Ferrel cell in January 2010, although certainly not weaker than in January 2007, is restricted to the latitude-band between from 30°N to 50°N. In fact, at θ=315 K, for example, the Ferrel cell in January 2010 is restricted to the latitude-band between 30°N and 48°N. Big differences between the negative NAM-phase and the positive NAM-phase in terms of the amplitude of eddy PVS- and eddy mass-fluxes fluxes are apparent especially in the latitude-band between 50°N and 60°N. The mass flux, $[v][\sigma]$, due to the secondary circulation in this latitude-band, i.e. the Ferrel cell, mostly weakens the net meridional mass flux in the positive NAM-phase, while it has little effect on the net meridional mass flux in the negative NAM-phase.

On a monthly time scale, both the PVS-flux, $[v][\zeta_a]$, and the mass flux, $[v][\sigma]$, due to the Ferrel cell, are very strongly anti-correlated with the eddy PVS-flux, $[v^*\zeta^*]$, as can be seen in **figures 5** and **8**. It must be reiterated that this effect is important especially in the latitude-band between 50°N and 60°N. At 50°N, for example, the January-mean meridional mass flux due to the Ferrel cell in the layer between the isentropic levels at 300 K and 330 K is always equatorward, except in two years, one of these being 2010. Note in **figure 8** that the Ferrel cell still exists (i..e. $[v][\sigma]<0$) when $[v^*\zeta^*]=0$, according to the best linear fit. This indicates that the Ferrel cell is not forced only by the *local* meridional eddy PVS-flux, but also probably by diabatic effects, such as radiative flux divergence, or by meridional eddy PVS-fluxes at a distance.

The strongest January-mean equatorward mass flux due to the Ferrel cell in the layer between θ=300 K and θ=330 K at 50°N was recorded in January 2007: -34 kg $m^{-1}K^{-1}s^{-1}$. The January-mean meridional mass flux in this layer due to eddies ($[v^*\sigma^*]$) at 50°N in the years 1979-2018 varies from about +60 to nearly +100 kg $m^{-1}K^{-1}s^{-1}$, i.e. is always poleward. This means that the net meridional mass flux at 50°N is indirectly weakened by meridional eddy PVS-fluxes, as can be seen in **figure 9**. Because the net meridional mass flux at 50°N is anti-correlated with the NAM-index at sea level (van Delden, 2023), intense meridional eddy PVS-fluxes in the Middleworld will "drive" the NAM into its positive phase. A weakening of this eddy PVS-flux forcing will not directly "drive" the NAM into its negative. More is needed for that, as we shall see in the next section.

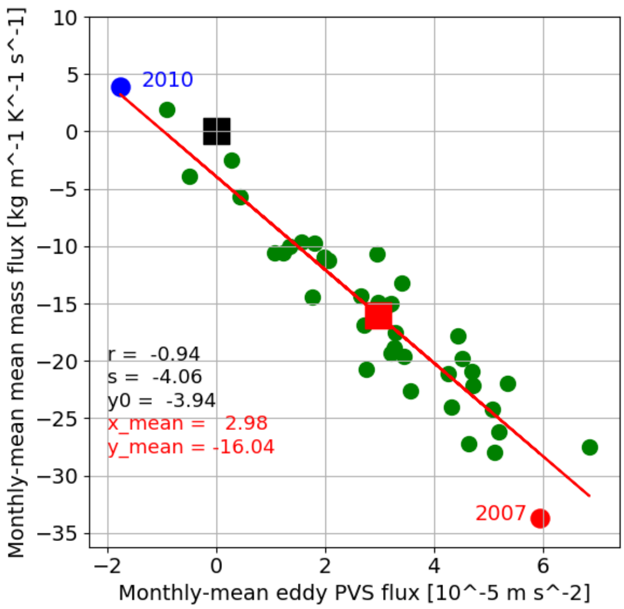

FIGURE 8. Scatter plot of the monthly average zonal-mean isentropic meridional mass-flux, $[v][\sigma]$, due to the secondary circulation in the layer between θ=300 K and θ=330 K and 50°N as a function of the monthly average zonal-mean *eddy* isentropic meridional PVS-flux, $[v^*\zeta^*]$, at θ=315 K and 50°N, for all months of January between 1979 and 2018. The red straight line, which represents the best linear fit to the 40 points (correlation coefficient is -0.94), does not go exactly through the origin (the black square). The red square represents the ensemble average value for all 40 months of January. The ensemble average eddy PVS-flux is $+2.98\times10^{-5}$ m s^{-2}. The ensemble average mean mass-flux is -14.26 kg m^{-1} K^{-1} s^{-1}. The blue dot is for January 2010 (extreme negative NAM-phase); the red dot is for January 2007 (extreme positive NAM-phase). Based on the ERA-Interim reanalysis (Dee et al., 2011).

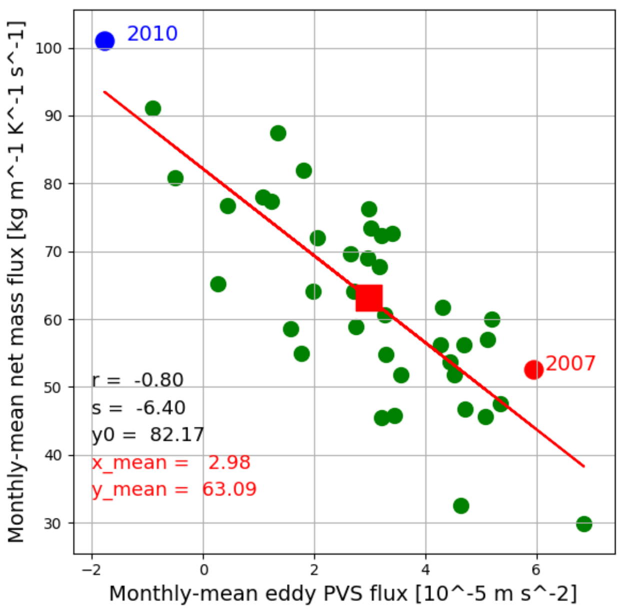

FIGURE 9. Scatter plot of the monthly average zonal-mean *net* (residual) isentropic meridional mass-flux, $[v\sigma]$, in the layer between θ=300 K and θ=330 K and 50°N as a function of the monthly average zonal-mean *eddy* isentropic meridional PVS-flux, $[v^*\zeta^*]$, at 315 K and 50°N, for all months of January between 1979 and 2018. The red straight line represents the best linear fit to the 40 points (correlation coefficient is -0.80). The red square represents the ensemble average value for all 40 months of January. The ensemble average eddy PVS-flux is $+2.98\times10^{-5}$ m s^{-2}. The ensemble average net mass-flux is +63.1 kg m^{-1} K^{-1} s^{-1}. The blue dot is for January 2010 (extreme negative NAM-phase); the red dot is for January 2007 (extreme positive NAM-phase). Based on the ERA-Interim reanalysis (Dee et al., 2011).

7. Analysis of a NAM-phase transition

Because net advective meridional PVS-fluxes and accompanying intensity-changes of the circumpolar primary circulation in the Northern Hemisphere are small in a typical month of January, the monthly mean circumpolar primary circulation in January is always in close gradient wind balance. That is why PV-inversion works on monthly mean PV-fields, as is demonstrated van Delden and Hinssen (2012) (see also section 5 of van Delden, 2023). Nevertheless, the monthly average intensity of the primary circulation varies appreciably between months of January in different years. This is because the monthly average primary circulation is the net result of averaging periods of time, or "events", in which the atmosphere is "locked", by positive feedback loops, into one of the two NAM-phases, or is transitioning from one NAM-phase to the other. Such transitions take time. January 2007, for example, which is labeled as an extreme positive NAM-phase month, actually consists of two NAM-events and a week-long transition between these two events. The intense positive NAM-event, which gave January 2007 its label, "extreme positive NAM-month", was followed on day 18 by a transition to a negative NAM-event. This negative NAM-event is one of the 38 negative NAM-events, which were used by Riviere and Drouard (2015) to derive a composite negative NAM-event. The composite negative NAM-event, in which the NAM-index is one standard deviation below average, lasts 12 days.

On the basis of a case study of the NAM-phase transition that occurred at the end of January 2007, this section discusses the important physical processes that govern a NAM-phase transition, in particular the processes that govern the transition from the positive NAM-phase to the negative NAM-phase.

The central date of the negative NAM-event, which is under investigation here, is 25 January 2007 (Riviere and Drouard, 2015). The transition to this negative NAM-event started about week earlier. The transition from one NAM-phase to the opposite NAM-phase, indeed, is not like crossing a tipping point in a non-linear physical system, rather it is a consequence of a relatively slow cumulative process associated with persistent meridional fluxes of vorticity or of mass in middle latitudes. This idea was shown by Hinssen and Ambaum (2010) to apply also to the occurrence of Sudden Stratospheric Warmings (SSW's).

By the cumulative effect of either persistent anomalous mass fluxes or persistent anomalous PVS-fluxes, or both, the middle latitude atmosphere is gradually pushed out of a positive feedback loop that held it locked in an extreme NAM-phase. If circumstances are favourable, the middle latitude atmosphere is subsequently driven and locked into the opposite extreme NAM-phase and its associated positive feedback loop. In the case of the NAM-phase transition, which occurred after 18 January 2007, the zonal mean eddy PVS-flux decreased from an average of nearly $+10^{-4}$ m s^{-2} in the first 18 days of January 2007 to negative values between 19 and 24 January 2007 (**figure 10**).

A relatively intense and long-lasting poleward mass flux pulse is also observed between these dates, coinciding with a decrease of the dimensional NAM-index from +10 hPa to -1 hPa. The dimensional NAM-index is defined here simply as the zonal-mean pressure difference at sea level between 35°N and 65°N relative to the 40 year daily January-climatology of the zonal-mean pressure difference at sea level between 35°N and 65°N. Consistent with earlier findings, the STJ-intensity, defined as the maximum value of $[u]$ in the Middleworld, exhibits a step-like increase in time of 10 m s^{-1} between 19 and 21 January, which indicates an increase of the zonal-mean baroclinicity in the sub-tropics (see figure 11 in van Delden, 2023). Simultaneously, the zonal-mean zonal wind velocity, $[u]$, at 50°N decreases by about 15 m s^{-1}.

What process initiated or forced this NAM-phase transition in January 2007? The Hovemöller diagram in **figure 11** provides some clues. It shows the instantaneous meridional isentropic mass flux, $v\sigma$, at 50°N in the layer between θ=300 K and θ=330 K as a function time and longitude for the month of January 2007. The meridional mass flux, $v\sigma$, is calculated from the pressure at θ=300 K and θ=330 K and the meridional velocity at θ=300 K 315 K and 330 K according the numerical approximation,

$$v\sigma \approx -0.25 \times \left(2v_{315} + v_{300} + v_{330}\right) \times \left(p_{330} - p_{300}\right)/(30g).$$

The subscript indicates the potential temperature. Isentropic density is defined in eq. 3.

Alternating poleward and equatorward mass flux pulses are observed in **figure 11**, which last a few days between initial growth and final decay. These features represent eastward travelling baroclinic planetary waves, which grow at preferred longitudes due to baroclinic instability, propagate eastward and decay at different preferred longitudes. Wave amplitude-growth is manifest as an intensifying pulse of poleward mass flux, indicated by red shading in **figure 11**, occurring especially over the Western Atlantic

Ocean and over the Central Pacific Ocean. The zonal phase speed of these pulses of poleward mass flux, which last about 3 to 6 days, is eastward and appears to depend on the zonal wavelength of the wave. Before January 20th, the number waves observed along a parallel is 5-7. January 20th marks a rather sudden transition to a lower wave number range (3-4) and much slower eastward wave propagation. The amplitude-decay of the pulses of poleward mass flux is accompanied, with a certain time lag, by a pulse of equatorward mass flux appearing in advance (downstream) of the original pulse of poleward mass flux.

The wave-like features in the meridional isentropic mass flux, seen in **figure 11**, are manifestations of planetary waves, travelling along the circumpolar wave guide (Branstator, 2002), formed by the mainly poleward potential vorticity gradient. These planetary waves undergo baroclinic wave life cycles with life times of about 3 days before the transition on January 20th, and considerably longer life times after this transition. For example, over the Pacific Ocean one baroclinic life cycle can be observed, starting on 11-12 January, with a pulse of poleward mass-flux at 160°W. This feature travels eastward, reaching the longitude of 110°W on 16 January. This is equivalent to a distance of about 3500 km in about 4.5 days, i.e. a speed of 9 m s^{-1}. Between 5 and 10 January the eastward phase speed of the features in the meridional mass flux over the Atlantic Ocean is much faster: approximately 15 m s^{-1}. Nevertheless, because the zonal-mean zonal wind velocity at 50°N, in the first 18 days of January 2007, in the layer θ=300-330 K, is in the order of 20 m s^{-1}, even the shortest waves propagate westward with respect to the mean flow, as is expected from the dispersion relation for barotropic Rossby waves (Holton, 2004, eq. 7.91).

The "wave-regime transition" at 50°N on January 20th in the layer between θ=300 K and θ=330 K starts in the Central to East Pacific Ocean, and subsequently propagate eastwards and weakening over North America while propagating into the Atlantic and re-intensifying there (**figure 11**). After January 20th pulses of poleward mass flux exceed 5000 kg s^{-1} m^{-1} K^{-1} for days at a fixed longitude, i.e. with negligible zonal displacement. These pulses presumably are associated with significant sea-level pressure rises poleward of 50°N. The poleward mass flux pulses usually exceed the equatorward mass flux pulses in magnitude. This means that the net mass flux is poleward, as can be verified in **figure 10**.

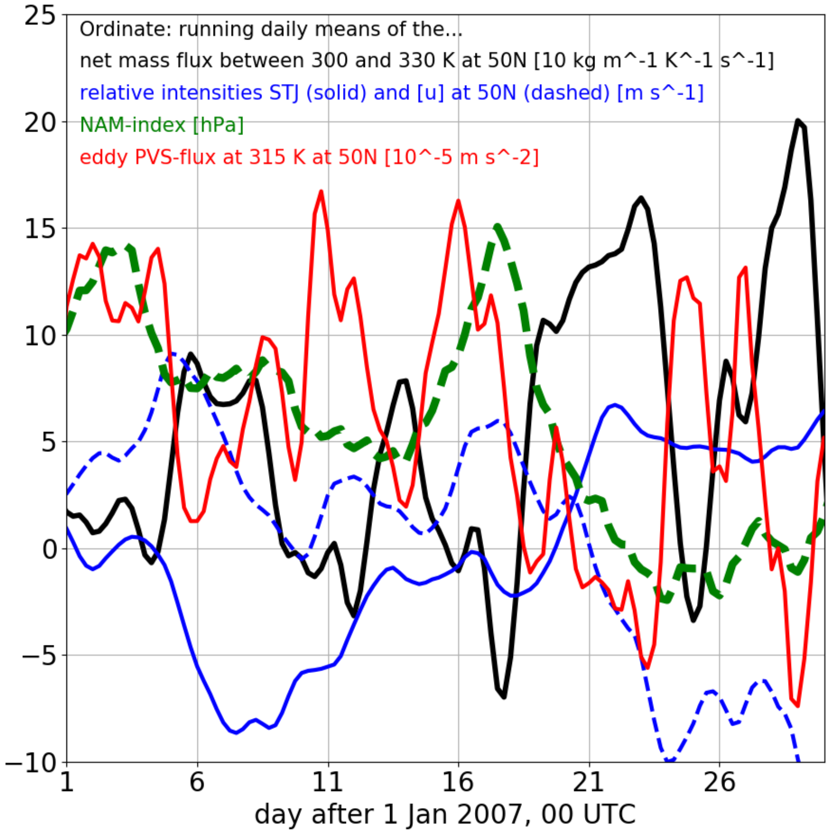

FIGURE 10. Running daily mean zonal-mean net isentropic meridional mass flux at 50°N in the layer between θ=300 K and θ=330 K in units of 10 kg $s^{-1}m^{-1}K^{-1}$ (black curve), intensity of the Sub-Tropical Jet (STJ) (blue, solid) (m s^{-1}) relative to the monthly mean in January 2007 (42.8 m s^{-1}), the zonal-mean zonal wind, [*u*], at 50°N and θ=315 K (blue, dashed) (m s^{-1}) relative to the monthly mean in January 2007 (19.6 m s^{-1}), NAM-index (green, dashed) (hPa) and eddy PVS-flux (red) (10^{-5} m s^{-2}) at θ=315 K as a function of the day in January 2007. See also **figure 4** in part 1 of this paper (van Delden, 2023). A transition from a positive NAM-event, with strongly positive (poleward) eddy PVS fluxes, a relatively weak STJ and weak meridional mass flux, to a negative NAM-event, with strongly mostly negative eddy PVS fluxes, a relatively intense STJ and intense meridional mass flux, took place in the week after 18 January 2007. Based on ERA-Interim reanalysis (Dee et al., 2011).

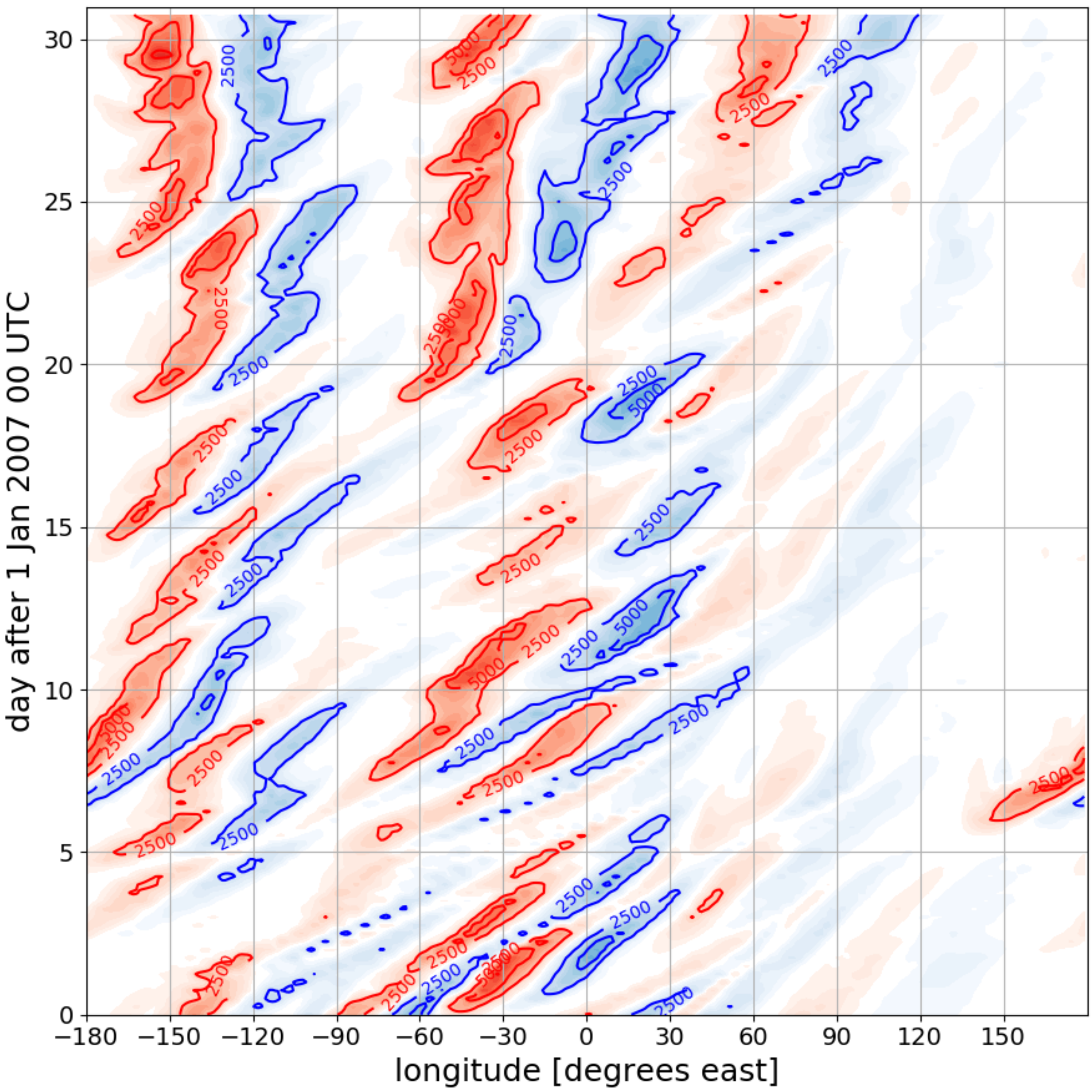

FIGURE 11. Meridional component of the isentropic mass flux at 50°N in the layer between between θ=300 K and θ=330 K as a function of time and longitude. Red shading corresponds to northward mass flux, blue shading corresponds to southward mass flux. Absolute values of mass fluxes are labeled in units of kg $s^{-1}m^{-1}K^{-1}$. Based on the ERA-Interim reanalysis (Dee et al., 2011).

8. Conclusion

The Northern Annular Mode (NAM), which is most intense in winter, has two extreme phases: a negative phase and a positive phase. The two extreme NAM-phases are associated with positive feedback loops, associated, respectively, with meridional mass transfer and with meridional advective vorticity transfer.

The first positive feedback loop, which is the subject of the present paper, is associated with two properties of meridional advective vorticity fluxes due to eddies. First, vorticity acts as the density of a substance, which remains on isentropic surfaces, i.e. isentropic surfaces are impermeable to vorticity. Second, meridional eddy transfer of vorticity is up the background meridional vorticity gradient. The background meridional vorticity gradient is determined to a large degree by the positive poleward planetary vorticity gradient. Vorticity in middle latitudes, therefore, is transferred poleward along isentropic surfaces by eddies, thereby intensifying both the zonal-mean zonal wind and the meridional vorticity gradient, hence further increasing the poleward eddy vorticity flux. This positive feedback loop governs the positive NAM-phase. An important side-effect to this feedback loop has to do with the fact that the atmosphere responds to the meridional eddy vorticity flux by producing a secondary meridional overturning circulation (the Ferrel cell), which opposes the eddy-effect in terms of both meridional flux of vorticity- and and the meridional flux of mass. In the Middleworld the meridional mass flux due to the secondary circulation opposes the mostly poleward eddy mass flux and so helps to prevent a transition to the negative NAM-phase, which is associated with an intense poleward mass flux in the Middleworld, as is summarized below.

The second positive feedback loop, which is subject of the previous part of this paper (van Delden, 2023), is associated with poleward isentropic mass fluxes in the Middleworld. The zonal-mean meridional divergence of the isentropic mass flux due to eddies in the Middleworld in the lower middle latitudes intensifies the zonal-mean baroclinicity and the associated subtropical jet (STJ), and hence also the associated available potential energy, which feeds more eddies, which, in turn, will continue to push more mass poleward. This positive feedback loop is described in some detail in part 1 of this paper, without going into the details of the separate roles of eddies and the secondary circulation. The present paper (part 2) adds an interesting side-effect to this feedback loop. The intense STJ is associated on its poleward side, between 45°N and 55°N, with a reduced poleward vorticity gradient, and in view of the **figure 7**, also with relatively weak poleward eddy vorticity fluxes, which prevents a poleward expansion of the Ferrel cell, thus also preventing a transition to the positive NAM-phase.

These feedback loops seem to depend on the scale of eddies. The first feedback loop operates when waves are relatively short (wave numbers 5-7); the second feedback loop operates when waves are long (wave numbers 3-4) and relatively stationary in the zonal direction. The question what determines the wavelength of planetary waves in middle latitudes remains open. Riviere and Drouard (2015) have shown that NAM-anomalies are triggered by anomalous convection in the western tropical Pacific. A case study of a transition from the positive to the negative phase indicates that this transition is associated with an increase of the horizontal scale of the eddies, which is indeed first visible in middle latitudes over the Pacific Ocean and spreads eastwards over North America, into the North Atlantic Ocean and then to Eurasia.

9. Acknowledgments

This paper is a follow-up of a workshop on the Northern Annular Mode held at IMAU (Utrecht University) on 19 April 2018. I thank the presenters (Maarten Ambaum, Frank Selten, Annalisa Cherchi, Wim Verkley, Wim van Caspel and Bob Ammerlaan) for their presentations and all participants for their contributions to discussions.

10. List of symbols

c_p: specific heat at constant pressure (=1004 J $kg^{-1}K^{-1}$)
f: Coriolis parameter or planetary vorticity=$2\Omega\sin\phi$.
g: acceleration due to gravity (=9.81 m s^{-2})
$\vec{I}$: mass flux vector (equation 7)
$\vec{J}$: vorticity (PVS) flux vector (eq. 5)
p: pressure
p_{ref}: reference pressure (=10^5 Pa)
T: temperature
u, v: zonal and merdional velocity
u_{gr}: gradient (balanced) wind
x, y, z: zonal, meridional and height coordinate
Z_θ: isentropic potential vorticity (eq. 1)
ζ, ζ_a: relative vorticity, absolute vorticity (ζ_a=f+ζ)
θ: potential temperature (eq. 1)
λ, ϕ, : longitude, latitude,
σ: isentropic density (eq. 3)
Ψ: isentropic streamfunction (Ψ=c_pT+gz)
Ω: earth's angular velocity= 7.3×10^{-5} s^{-1}

11. References

Ambaum, M.H.P., 1997: Isentropic formation of the tropopause. **J.Atmos.Sci**., **54**, 555-568.

Balasubramanian, G. and S. Garner, 1997: The Role of Momentum Fluxes in Shaping the Life Cycle of a Baroclinic Wave. **J.Atmos.Sci. 54**, 510-533.

Bennedict, J.J., S. Lee and S.B. Feldstein, 2004: Synoptic view of the North Atlantic Oscillation. **J.Atmos.Sci.**, **61**, 121-144

Branstator, G, 2002: Circumglobal Teleconnections, the Jet Stream Waveguide, and the North Atlantic Oscillation. **J.Clim., 15**, 1893-1910.

Butchart, N., 2014: The Brewer-Dobson circulation, **Rev. Geophys., 52,** 157–184.

Charney, J., 1971: Geostrophic turbulence. **J.Atmos.Sci. 28**, 1088-1095.

Delden, A.J. van, and Y.B.L. Hinssen, 2012: PV-theta view of the zonal mean state of the atmosphere. **Tellus A, 2012, 64**, 18710, https://a.tellusjournals.se/articles/10.3402/tellusa.v64i0.18710.

Delden, A.J. van, 2023: Physics of the Northern Annular Mode - Part 1: connection to meridional mass transfer. **Annals of Geophysics**, submitted

Dima, I.M., and J.M. Wallace, 2003: On the seasonality of the Hadley cell. **J.Atmos.Sci., 60**, 1522-1527.

Dee, D. et al., 2011: The ERA-Interim reanalysis: configuration and performance of the data assimilation system. **Quart.J.R.Met.Soc., 137**, 553-597. (https://doi.org/10.1002/qj.828)

Eliassen, A., 1951: Slow thermally or frictionally controlled meridional circulation in a circular vortex. **Astrophysica Norvegica, 5**, 19-60.

Haynes, P.H., and M.E. McIntyre, 1987: On the evolution of voorticity and potential vorticity in the presence of diabatic heating and frictional or other forces. **J.Atmos.Sci.**, **44**, 828-841.

Haynes, P.H., and M.E. McIntyre, 1990: On the conservation and impermeability theorems for potential vorticity. **J.Atmos.Sci.**, **47**, 2021-2031.

Hinssen, Y. B.L. and Ambaum, M.P.H., 2010: Relation between the 100 hPa heat flux and stratospheric potential vorticity. **J.Atmos.Sci.**, **67**, 4027-4027.
Kuo, H-L., 1951: Vorticity transfer as related to the development of the general circulation. **J.Atmos.Sci., 8,** 307-315.

Holton, J.R., 2004: **An Introduction to Dynamic Meteorology**, Fourth Edition. Elsevier Academic Press. 529 pp.

Kuo, H-L., 1956: Forced and free meridional circulations in the atmosphere. **J.Atmos.Sci., 13**, 561-568.

Li, J., and J.X.L. Wang, 2003: A modified zonal index and its physical sense. **Geophys.Res.Lett., 30**, 1632.

Plumb, R.A., and J. Eluszkiewicz 1999: The Brewer-Dobson circulation: Dynamics of tropical upwelling. **J.Atmos.Sci., 56**, 868-890

Riviere, G., and M. Drouard, 2015: Dynamics of the Northern Annular Mode at Weekly Time Scales. **J.Atmos.Sci., 72,** 4569-4590.

Starr, V.P., 1948: An essay on the general circulation of the earth's atmosphere. **J.Atmos.Sci.**, **5**, 39-43.

Starr, V.P., 1968: **Physics of Negative Viscosity Phenomena.** MacGraw-Hill, 256 pp.

Thorncroft, C.D., B.J.Hoskins and M.E.McIntyre, 1993: Two paradigms of baroclinic-wave life-cycle behaviour. **Q.J.R.Meteorol.Soc., 119**, 17-55.